PETROLEUM EXPLORATION AND DEVELOPMENT
Volume 44, Issue 3, June 2017
Online English edition of the Chinese language journal

Available online at www.sciencedirect.com
ScienceDirect

Cite this article as: PETROL. EXPLOR. DEVELOP., 2017, 44(3): 446–453.

RESEARCH PAPER

A numerical simulation model for multi-scale flow in tight oil reservoirs

FANG Wenchao[1, 2], JIANG Hanqiao[1], LI Junjian[1, *], WANG Qing[3], KILLOUGH John[2], LI Linkai[1], PENG Yongcan[3], YANG Hanxu[1]

1. Department of Petroleum Engineering, China University of Petroleum (Beijing), Beijing 102249, China;
2. Texas A&M University, College Station 77840, USA;
3. Research Institute of Petroleum Exploration and Development, PetroChina Xinjiang Oilfield Company, Karamay 834000, China

Abstract: A discrete fracture model for multi-scale flow in large-scale fractured tight oil reservoirs is proposed considering the compressibility of reservoir rock and fluid, and the non-linear flow in the tight matrix. Validation of the model is performed, followed by the field application of the model. The two-point flux-approximation scheme is adopted in the model to calculate conductivity, and small grids at the fracture intersections are eliminated by the "star-delta" transformation method to improve the computational stability. The fully implicit discretization scheme is performed on the temporal domain. Automatic differentiation technique which can improve model establishment efficiency and computational accuracy is applied in the model to solve the numerical model. The model is validated with the simulation results of Eclipse and the historical production data of a long fractured horizontal well in a tight oil reservoir in Xinjiang oilfield. Simulation results of a field-scale reservoir show that the model proposed can simulate reservoirs with large-scale complex fracture systems; well productivity is positively correlated with the scale of the stimulated reservoir volume, and the difference in planar fracture density and fracture connectivity are proved to be the key factors that lead to the heterogeneous distribution of remaining oil in tight oil reservoirs.

Key words: tight oil reservoir; discrete fracture model; multi-scale coupling; fracture network; volume fracturing

Introduction

The dual-continuum model and local refine PEBI grid model in Eclipse are two main models used for simulating fractured reservoirs in commercial numerical simulators at present. The double media model is applied in Logarithmically Spaced, Locally Refined, and Dual Permeability model (LS-LR-DK)[1–2] of CMG-GEM and the whole grid logarithm refine model[3] of Nexus. The dual media models in CMG-GEM and Nexus, both taking continuous and large-scale orthogonal simplification method to describe fractures, can't characterize the discrete features of fractures in the reservoir. The PEBI grid model in Eclipse, although capable of describing discrete fractures, is less adaptable to small-scale fractures and large-area fracture network systems[4]. In addition, the dual (and multiple) media model has some inherent disadvantages[5–7]. For these reasons, numerical simulation methods for discrete fractures have been a study focus of researchers. There are some preliminary methods proposed by foreign researchers, but all based on the assumption that rock and fluid in reservoir are incompressible, only capable of handling small scale fracture system and a small number of fractures, and adopting Darcy law for conventional reservoir to simulate flow law of fluid in matrix, these methods are not suitable for simulation of large-scale complex fracture systems in tight oil reservoirs[8–10]. Meanwhile, research in this area is still relatively inadequate in China.

In this study, a discrete fracture numerical simulation model for multi-scale flow in tight oil reservoirs considering the compressibility of reservoir rock and fluid, and non-linear flow in matrix is proposed. "Star-delta" transformation method is introduced into this model to calculate transmissibility, and automatic differential (*AD*) method is used in the solution module. The model has been validated by the simulation results of Eclipse and a fractured horizontal well located in a tight oil reservoir in Xinjiang oilfield. Finally, the model was used to simulate a tight reservoir with large-scale complex fracture network in the "factory well pad" operation mode of Xinjiang oilfield.

1. Multi-scale flow theory

Composed of tight matrix and fracture, the tight reservoir

Received date: 28 Jun. 2016; **Revised date:** 22 Mar. 2017.
*** Corresponding author.** E-mail: junjian@126.com
Foundation item: Supported by the National Key Basic Research and Development Program (973 Program), China (2015CB250900).

shows multi-scale characteristic, including differences in size and spatial distribution of the two media[11], differences of mass flow rate in time scale[12]; and differences in mechanism of mass transfer in different media. Therefore, special characterization method for multi-scale flow is needed for simulation of this kind of complex multi-scale reservoir.

The fractures in reservoir should be characterized by unstructured grids since the existence of fractures makes the spatial distribution of media highly discontinuous, and regular structured grids can't meet the requirements. Moreover, the huge difference in size between the matrix and the fracture is bound to bring great challenge to the calculation stability, so in this study, special methods of gridding such as reduced dimension of fractures was adopted to avoid forming small grids when gridding in tiny fractured space.

The different velocities of fluid flow in the matrix and fracture, and the randomness of the unstructured grid connectivity make it impossible to calculate the system transmissibility with one uniform method. Therefore, the half transmissibility correction method for a single grid was used to calculate the transmissibility of different porous media, and then the control volume two-point flow approximation (TPFA) method and "star-delta" transformation method were adopted to calculate the total transmissibility of different types of connections (matrix-matrix, matrix-fracture, fracture-fracture), to reflect the coupling of all different flows in the multi-scale porous media.

Different from Darcy flow in fracture, fluid flow in tight matrix shows obvious non-linear feature. To characterize the different flow mechanisms in different media, taking advantage of half transmissibility calculation method in different media, the non-linear flow in the matrix was characterized by modifying the half transmissibility of the matrix grid in this study, while the fluid flow in the fracture grid was simulated by Darcy flow, forming the calculation flow of total transmissibility considering differences and coupling of matrix-matrix, matrix-fracture and fracture-fracture transmissibilities.

2. Mathematical model

At present, the popular development mode of tight oil reservoir is depletion development relying on the elasticity of rock and fluid. Therefore, rock and fluid compressibility are considered in this mathematical model. The continuity equation is written as:

$$\frac{\partial(\rho\phi)}{\partial t}+\operatorname{div}(\rho \boldsymbol{v})=q_{\mathrm{v}} \tag{1}$$

Mathematical models of compressible rock and fluid are expressed as:

$$\phi(p)=\phi_0 \mathrm{e}^{C_{\mathrm{r}}(p-p_0)} \tag{2}$$

$$\rho(p)=\rho_0 \mathrm{e}^{C_{\mathrm{o}}(p-p_0)} \tag{3}$$

The matrix in tight oil reservoir, containing micro-nano-pores, has apparent micro-scale effect[13–14]. Considering the fluid boundary layer and the yield stress, the non-linear flow in the matrix is described by the following equation[15]:

$$\boldsymbol{v}_{\mathrm{m}}=-\frac{K}{\mu}\ \mathbf{grad}\ p\left(\frac{m}{m+|\mathbf{grad}\ p|}-1\right) \tag{4}$$

The fluid flow in the fracture still followed the classical Darcy law.

Peaceman's model used universally in the current commercial numerical simulator was adopted as well model[16].

3. Gridding method

The target area is divided into unstructured grids using the constrained Delaunay triangulation[17–18] (Fig. 1). The flexibility of the triangular grid shape allows the subdivision module to handle various complex distributed fractured networks.

The fractures in the grid domain of Fig. 1 are treated as one-dimensional line grids. Dimension reduction of fracture is a key approach to improve the efficiency and stability of multi-scale simulation. If the fractures are considered as two-dimensional in the grid system, they will be triangulated in the fracture space with very small width, generating many small grids, making the subsequent solving process very difficult. Juanes et al.[19] found through study that the simulation had much higher computational convergence in which the fractures were taken as one-dimensional than that in which the fractures were taken as two-dimensional.

4. Numerical solving method

4.1. Calculation method of multi-scale transmissibility

The main purpose of discrete space in mathematical model is to calculate spatial transmissibility. For any grid shape, the spatial mass transfer between adjacent grids can be described as follows:

$$q_{ij}=T_{ij}\frac{\rho}{\mu}\left(p_j-p_i\right) \tag{5}$$

Using the TPFA method, the expression for T_{ij} can be deduced[20]:

$$T_{ij}=\frac{T_i T_j}{T_i+T_j} \tag{6}$$

T_{ij} is essentially the total transmissibility of adjacent grids, and its calculation adopted the concept of half transmissibility, that is, the transmissibility between single grid and grid inter-

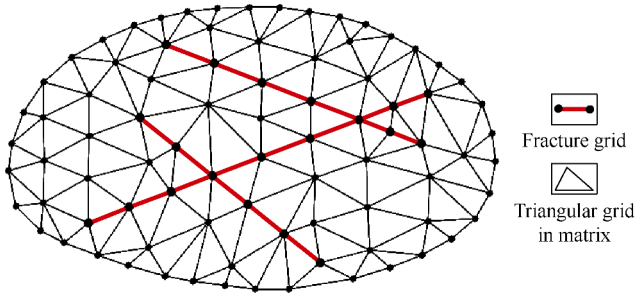

Fig. 1. Schematic diagram of constrained Delaunay triangulation.

face. When the flow obeys Darcy's law, the half transmissibility is calculated by:

$$T_i = \frac{A_i K_i}{D_i} \boldsymbol{n}_i \boldsymbol{f}_i \tag{7}$$

In the mixed-grid system, due to the non-linear characteristic of fluid flow in the matrix grid, the equation (7) needs to be modified:

$$T_i = K_i \left(\frac{m}{m + |\mathbf{grad}\ p|} - 1 \right) \frac{A_i}{D_i} \boldsymbol{n}_i \boldsymbol{f}_i \tag{8}$$

Equation (8) shows that the half transmissibility of the matrix grid is related to the grid pressure, and changes with time in the simulation process. Given any two matrix grids, the TPFA method can be used to calculate the total transmissibility between them. However, some special treatment is required when dealing with fracture grids.

4.1.1. Calculation of matrix-fracture transmissibility

In the triangular grid domain, the fracture is one-dimensional line element, while in the calculation domain, the fracture is restored to a two-dimensional grid with certain width to calculate the fluid mass transfer. After restored to a two-dimensional grid, the fracture grid is regarded as a common grid, and TPFA method is used directly to calculate the total transmissibility, and the half transmissibility of the fracture grid is expressed as:

$$T_i = \frac{2 A_{\mathrm{m,f}} K}{w_{\mathrm{f}}} \tag{9}$$

4.1.2. Calculation of fracture-fracture transmissibility

The intersection of two fracture grids is the simplest transfer form between different fracture grids (Fig. 2). When the fracture grids intersect, the mass transfer medium is no longer an interface, but an intermediate polyhedron. Due to the small fracture width, this intermediate grid is much smaller than other common grids. In reservoirs with abundant fractures, large numbers of these tiny grids will greatly reduce the stability of numerical simulation.

The transmissibility between the cell C_1 and C_2 can be expressed as a harmonic mean:

$$T_{12} = \frac{T_{01} T_{02}}{T_{01} + T_{02}} \tag{10}$$

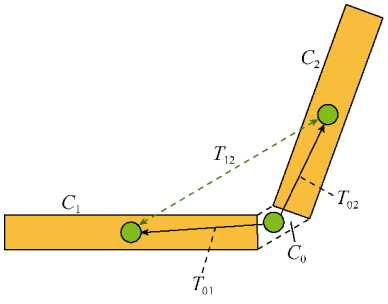

Fig. 2. Schematic diagram of transmissibility at the intersection of two fracture grids.

where T_{01} and T_{02} both contain the half transmissibility of the intermediate grid C_0. The information of intermediate is eliminated by using the following approximation method: for T_{01}, since D_1 is much larger than D_0, and K_1 is nearly equal to K_0, so T_1 is much smaller than T_0, then T_{01} is approximately equal to T_1 according to equation (6) and T_{02} is approximately equal to T_2. Therefore, equation (6) can be re-expressed as (where T_{12} denotes the non-adjacent grid full transmissibility):

$$T_{12} = \frac{T_1 T_2}{T_1 + T_2} \tag{11}$$

It can be seen from equation (11) that T_{12} does not contain any intermediate grid parameters.

For the case in which multiple fracture grids intersect, the "star-delta" equivalent transformation algorithm (Fig. 3) is introduced to convert the "star" connection with intermediate connection point to the “delta” connection without intermediate connection point. Based on the principle of water and electricity similarity, the "star-delta" transformation is applied to the calculation of transmissibility in the intersection of multiple fractures.

Based on the principle of water and electricity similarity, the "star-delta" transformation can be used to derive the mathematical expression for the transmissibility calculation combined with equation (11):

$$T_{ij} = \frac{T_i T_j}{\sum_{k=1}^{N_{\mathrm{f}}} T_k} \tag{12}$$

Equation (12) is the general formula of adjacent grids transmissibility calculation between fracture grids at any intersection number after the elimination of small grids at the intersection of.fractures

4.2. Full implicit discretization in time domain

In the time domain, the continuity equation is fully implicitly discretized:

$$\frac{(\rho\phi)_{n+1} - (\rho\phi)_n}{\Delta t_n} + \mathrm{div}(\rho \boldsymbol{v})_{n+1} = q_{n+1} \tag{13}$$

For the divergence term, the fluid density at the grid interface takes the average of fluid densities in the two grids. At the same time, the relationship between flow velocity and total transmissibility can be derived based on the TPFA method[21], and the final transformation of the equation is:

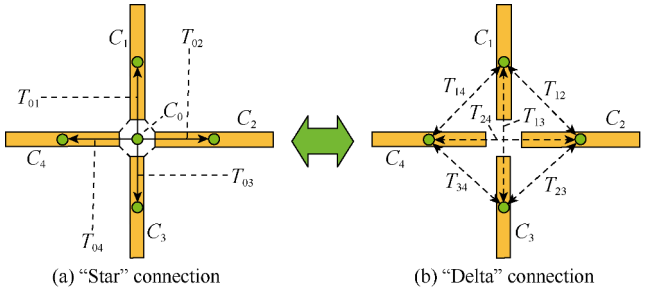

(a) “Star” connection (b) “Delta” connection

Fig. 3. Schematic diagram of "star-delta" transformation for calculating the transmissibility of multiple intersected fractures.

$$\frac{(\rho\phi)_{n+1}-(\rho\phi)_n}{\Delta t_n}+\mathrm{div}\left[-\mathrm{ave}(\rho_{n+1})\frac{T_{n+1}}{\mu}\mathbf{grad}\ p_{n+1}\right]=q_{n+1} \tag{14}$$

where div, ave and **grad** denote the divergence operator, mean operator and gradient operator respectively, collectively known as discrete operator[22–23]. The discrete operator functions between two grids in space. Therefore, when the geometric topology parameters of the grid domain are stored, the corresponding functions can be defined to describe the different discrete operators, and then the discrete operators are used to calculate the mass transfer parameters between the different grids in the whole grid domain, without the aid of complex parametric units (five or nine points) for calculation like traditional finite difference.

4.3. Automatic differentiation

The Newton iterative method is used to solve the numerical model. In the Newton iteration method, an equation containing unknown quantities is usually written as a margin form:

$$F(\boldsymbol{x})=0 \tag{15}$$

The iteration format is:

$$\begin{cases}\boldsymbol{x}_{n+1}=\boldsymbol{x}_n+\boldsymbol{\delta}_{n+1}\\ \boldsymbol{\delta}_{n+1}=-F(\boldsymbol{x}_n)\dfrac{1}{\boldsymbol{J}(\boldsymbol{x}_n)}\end{cases} \tag{16}$$

where $\boldsymbol{J}(\boldsymbol{x}_n)=\square F(\boldsymbol{x}_n)/\square(\boldsymbol{x}_n)$ is the Jacobian matrix.

Solving the Jacobi matrix is the most critical step in the Newton iteration method. Traditional methods include numerical differentiation or symbolic differentiation, which is time-consuming and error-prone. The SC-CFR model presented in this paper employs the automatic differential method[24–25] to calculate the Jacobian matrix.

The action variable of the automatic differential algorithm is not the traditional variable value, but data structure containing both the variable value and variable derivative, known as the *AD* variable. The first step in automatic differential programming is to define the meta-function *AD* variable, such as sin*a* corresponding to {sin*a*, cos*a*}, and finally form an *AD* variable class that contains all the basic meta-function *AD* variables.

Since the traditional arithmetic operator only operates on a single value, it is necessary to redefine the algorithm to perform *AD* variable computation:

$$\begin{cases}\{a,a'\}\pm\{b,b'\}=\{a\pm b,a'\pm b'\}\\ \{a,a'\}\times\{b,b'\}=\{ab,a'b+ab'\}\\ \dfrac{\{a,a'\}}{\{b,b'\}}=\left\{\dfrac{a}{b},\dfrac{a'b-ab'}{b^2}\right\}\end{cases} \tag{17}$$

The application of automatic differentiation can avoid complicated discretization of equation, and in the process of model establishment, the flow equation can be coupled into the model without changing the form of the equation, which greatly improves the efficiency of complex model building. At later stage when coupled with the new flow mechanism, it is not necessary to change the differential form of the equation extensively like traditional manual difference. Besides, truncation error results from replacing differential with differential quotient is also avoid, thus the accuracy and efficiency of the calculation are improved.

4.4. Multi-scale coupling calculation method

The multi-scale coupling calculation (Fig. 4) is an essential part of the numerical simulation model of discrete fractures in tight reservoirs, which mainly includes the coupling of half transmissibility between the media and inside the medium, and the coupling of nonlinear time-varying transmissibility (matrix nonlinear flow).

In the process of model application, the multi-scale coupling was divided into two systems for calculation. The half transmissibility in fracture system and the fracture-fracture total transmissibility are constant after the grid system is fixed and do not change with time. While the half transmissibility in matrix system and the matrix-fracture, matrix-matrix total transmissibility show non-linear changes over time, and need to be updated by calculation every step, resulting in the time-varying property of the total transmissibility in the whole multi-scale system.

5. Model validation

5.1. Validation by Eclipse

The same straight well double-wing fracture model was built in Eclipse and SC-CFR (Fig. 5), and local grid refinement method was used to generate fractures in Eclipse.

The parameters of the two simulators were the same: the original reservoir pressure of 20 MPa, matrix permeability of 0.1×10^{-3} μm^2, matrix porosity of 8%, fracture permeability of 30 m^2, and fracture width of 2.5 mm. Under the same conditions of fracture transmissibility, the locally refined grids have an equivalent fracture permeability of 0.187 5 m^2, fracture equivalent width of 400 mm, fracture porosity of 60%, rock

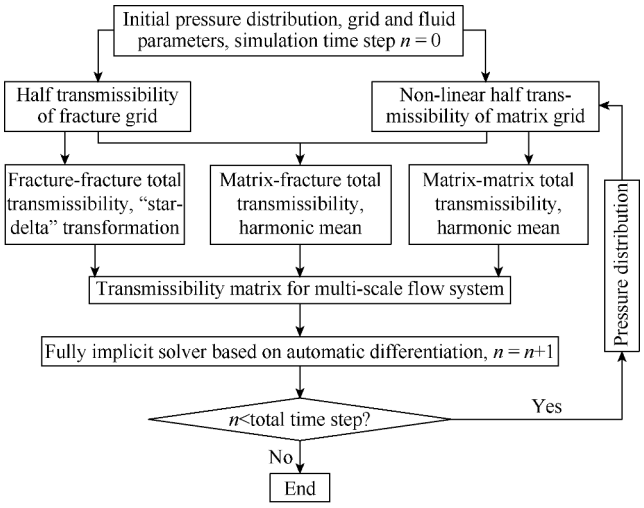

Fig. 4. Flow chart of multi-scale coupling calculation of tight reservoir.

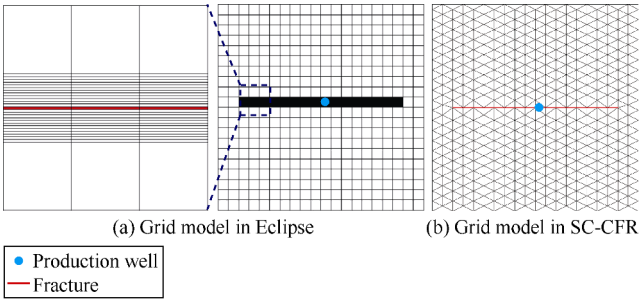

Fig. 5. Straight well double-wing fracture model created by two simulators.

compression coefficient of 1×10^{-5} MPa^{-1}, oil compression coefficient of 1×10^{-4} MPa^{-1}, oil viscosity of 5 mPa·s, in-situ oil density of 850 kg/m^3, and crude oil volume coefficient of 1.13.

Comparing the production data calculated by the two simulators (Fig. 6), we can see that the two simulators give highly consistent oil production and average reservoir pressure. Moreover, the plane pressure distribution at different time obtained by the two simulators are also compared (Fig. 7), except minor differences caused by grid direction effect, the pressure spread ranges and degrees simulated by two simulators have fairly good consistency.

The above comparison results show that SC-CFR has higher reliability.

5.2. Verification with field well

Well JT2-H is a multi-stage fracturing horizontal well in a tight oil reservoir of Xinjiang oil field, with a total lateral section of 1 026 m, designed fracturing stages of 15, and actual fracturing stages of 9 (Fig. 8). It started to produce oil from April 13, 2013, and had produced 4 632.05 m^3 of oil cumulatively as of July 2, 2015.

The reservoir of Well JT2-H has a pressure of 47.89 MPa, average matrix permeability of 0.4×10^{-3} μm^2, average matrix porosity of 7.3%, rock compression coefficient of 1×10^{-6} MPa^{-1}. The in-situ oil has a viscosity of 10.58 mPa·s, density of 924 kg/m^3, compression coefficient of 1×10^{-5} MPa^{-1}, and volume coefficient of 1.06.

Well JT2-H experienced three major events during production, shut-in in winter, overhaul, and transfer to pumping. It can be seen from the simulated production performance curve (Fig. 9) that the simulated results by SC-CFR are quite consistent with the actual production data, proving the nu-

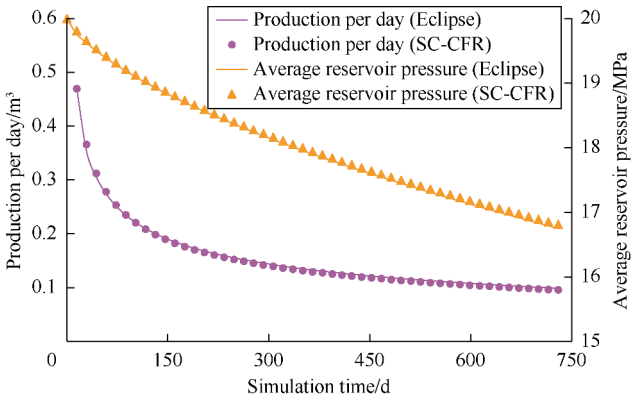

Fig. 6. Comparison of production data calculated by the two simulators.

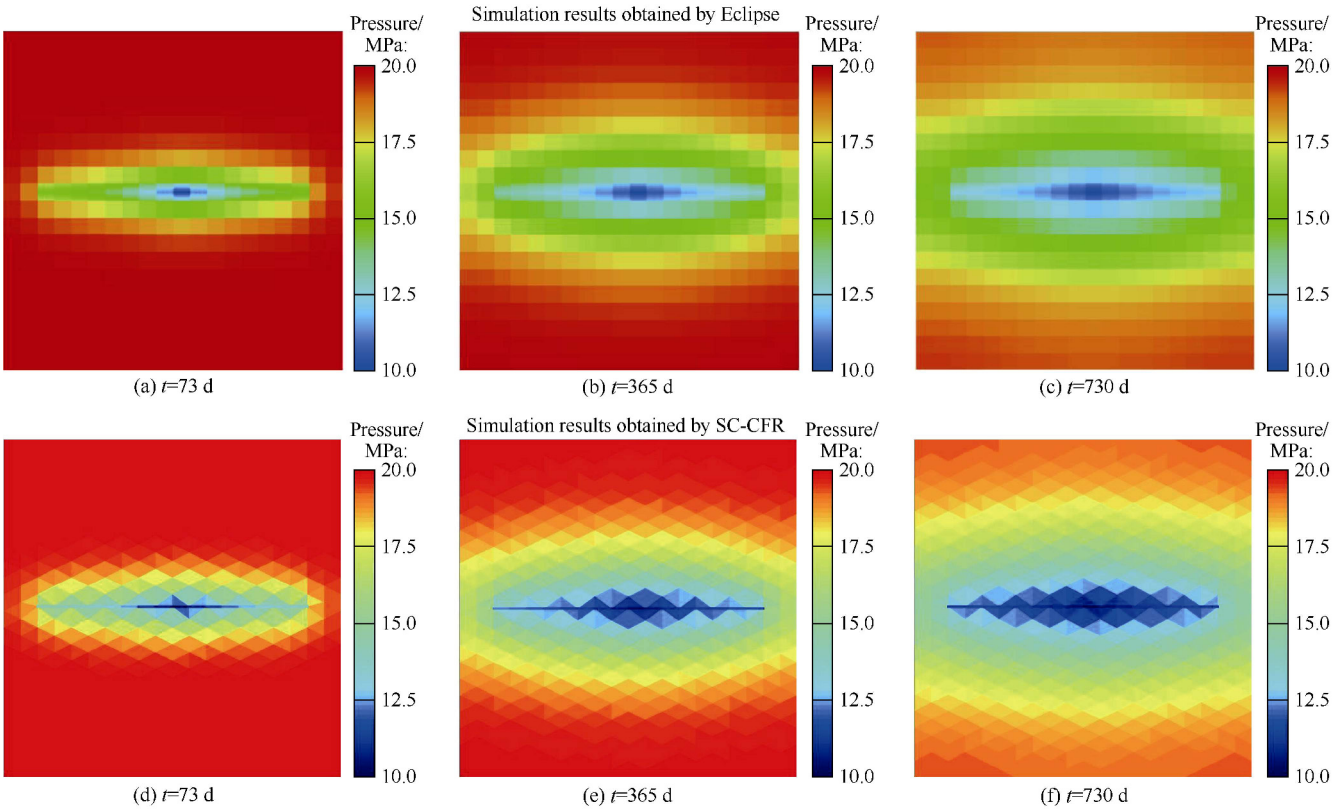

Fig. 7. Pressure distribution calcalated by the two simulators.

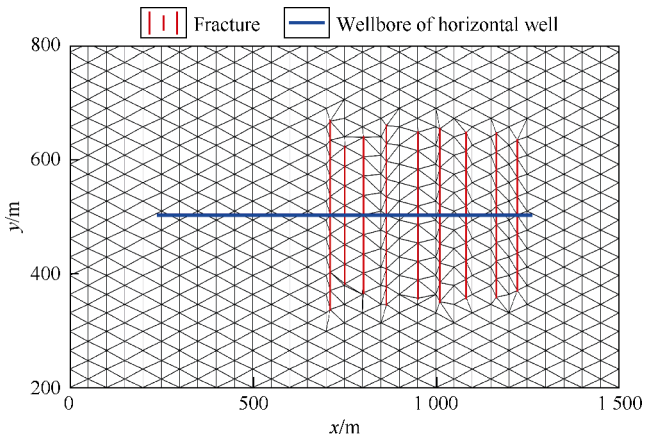

Fig. 8. The numerical simulation grid model of Well JT2-H.

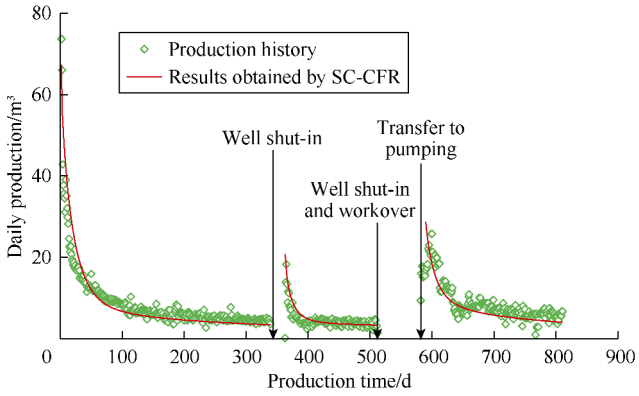

Fig. 9. Comparison of Well JT2-H production performance simulated by this model and historical performance.

merical simulation model proposed in this study has high reliability, and SC-CFR can simulate complex production process.

6. Application in large scale fracturing network

In order to further test the field application potential of SC-CFR, it was used to simulate a tight oil reservoir with large-scale fracturing network, and analyze the influence of fracturing network feature on the development of tight oil reservoir.

"Factory well pad" mode has been taken to develop tight oil reservoirs in Xinjiang Oilfield, that is, several long fractured horizontal wells from one well pad are designed to develop a tight reservoir in certain scope synergistically. A conceptual tight oil development pad model (Fig. 10) was designed by SC-CFR, which included three long volume fractured horizontal wells with lateral section of 2 600 m each. Different fracture densities were designed around the three wells, the number of fractures around Well A, B and C were 350, 250 and 150 respectively. The model had a matrix permeability of 0.1×10^{-3} μm^2, fracture width of 2.5 mm, original reservoir pressure of 20 MPa, and the other petrophysical and fluid parameters same as those of Well JT2-H in Xinjiang Oilfield. The simulation time is 1 825 d (5 a).

The production rates of the three wells simulated by SC-CFR are quite different (Fig. 11). The greater the density

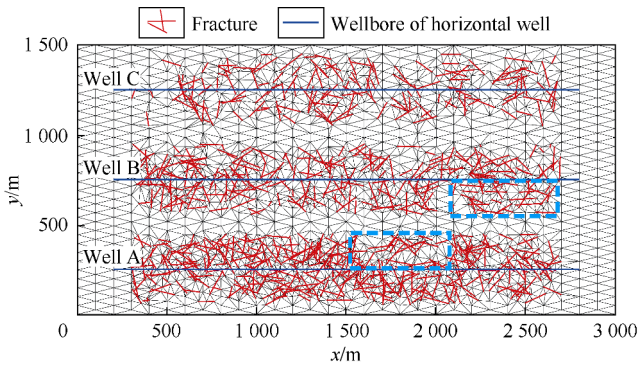

Fig. 10. Long volume fracturing horizontal well pad for tight oil reservoir development.

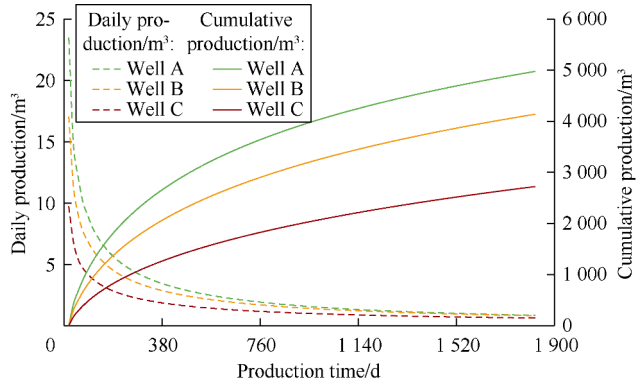

Fig. 11. Simulated production performances of three horizontal wells in the tight oil reservoir development pad.

of fracture network generated by the volume fracturing, the higher the productivity of the related horizontal well. But the difference in production mainly occurs in the early stage because the output is mainly from fractures at this time, and the production rates of the three wells have little difference in late period when the matrix becomes the main source of oil supply. In addition, the higher the initial production, the larger the production decline is.

Then we analyzed the plane production characteristics of the reservoir (Fig. 12). It can be seen from Fig. 12, the more the fractures around the horizontal well, the larger the stimulated area, and the higher the broken degree of reservoir is, so the greater the producing scope and degree, the higher the production will be. Therefore, in a reasonable economic range, the hydraulic fracturing should pursue bigger and denser fracture stimulated area.

In addition, the heterogeneity of the reservoir planar producing is closely related to the distribution of fractures. The higher the fracture density and the better the transmissibility of an area, the higher the producing degree of the area will be. For example, the 1 600–2 100 m zone in the horizontal direction of Well A has much smaller fracture density than other zones (Fig. 10), so this zone has lower producing degree (Fig. 12). Some areas have high fracture density but poor fracture connectivity, and also low producing degree. For example, the area below 2 200–2 600 m in horizontal direction of Well B (Fig. 10), although the fractures are dense, but are nearly par-

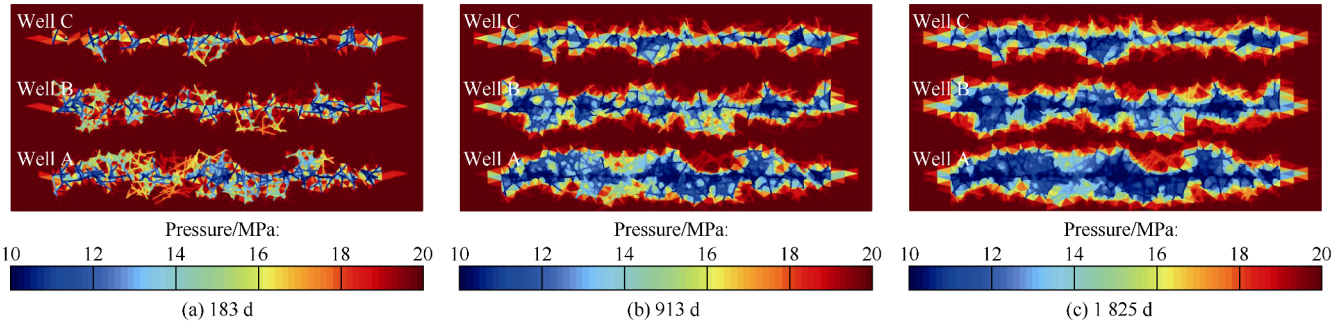

Fig. 12. Evolution of planar producing features of tight reservoir with time.

allel to each other, so the area has very low producing degree too (Fig. 12). In conventional sandstone reservoirs, the heterogeneity of residual oil distribution is dependent upon the permeability heterogeneity, but it is much different in volume fractured tight oil reservoir. It can be seen from the analysis above that the heterogeneity of the remaining oil in the tight oil reservoir is mainly dependent on the heterogeneity of the fracture density and the fracture network connectivity.

7. Conclusions

A discrete fracture model for fractured tight oil reservoir considering multi-scale flow characteristic, the compressibility of reservoir rock and fluid, and the non-linear flow in the tight matrix, has been established. In the model, TPFA method is adopted to evaluate multi-scale (matrix-matrix, matrix-fracture, fracture-fracture) transmissibility; the "star-delta" transformation method is used to eliminate tiny grids at the intersection of fractures to improve computational stability; and automatic differentiation technique is applied to solve the Jacobian matrix. The model has been validated by the simulation results of Eclipse and the historical production data of a long fractured horizontal well located in a tight oil reservoir in Xinjiang oilfield.

In line with the "factory well pad" development mode of tight oil reservoir in Xinjiang oilfield, simulations were performed on a development well pad model with three long fractured horizontal wells. The simulation results indicate that the simulator proposed in this study performs well in simulating large-scale complex fractured network. In addition, well productivity is found to be positively correlated with the scale and density of the stimulated reservoir volume; and the heterogeneous distribution of fracture density and fracture interconnectivity are proved to be the key factors leading to the heterogeneous distribution of remaining oil in tight oil reservoirs.

Nomenclature

a, b—variables;

a', b'—the derivatives of the variables;

A—the area of the grid contact surface, m^2;

$A_{m,f}$—the interfacial area of matrix grid and fracture grid, m^2;

C_o—the coefficient of fluid compressibility, Pa^{-1};

C_r—the coefficient of rock compressibility, Pa^{-1};

D—the distance between the center point of the grid and the contact surface, m;

$\boldsymbol{f}$—the vector pointing to the center point of the grid by the center point of the grid contact surface;

$\boldsymbol{J}(\boldsymbol{x}_n)$—the unknown vector x of the Jacobian matrix;

K— permeability, m^2;

m—the coefficient of non-linear flow, Pa/m;

n—time step;

$\boldsymbol{n}$—the unit normal vector on the grid contact surface;

N_f—the number of fracture grids at the same point;

p—the pressure, Pa;

p_0—the reference state pressure, Pa;

grad$p$ —the pressure gradient, Pa/m;

q_{ij}—mass transfer rate between C_i and C_j (C_i and C_j are a certain grid), kg/s;

q_v—the inflow/ outflow per unit volume, kg/(m^3·s);

t—the simulation time;

T_i—the half transmissibility of C_i (a certain grid), m^3;

T_j—the half transmissibility of C_j (a certain grid), m^3;

T_{ij}—the total transmissibility of C_i and C_j, m^3;

$\boldsymbol{v}$—the vector of flow velocity, m/s;

w_f—fracture width, m;

$\boldsymbol{x}$—unknown vector;

x, y—rectangular coordinate;

$\boldsymbol{\delta}$—Newton iteration residual;

Δt—time step;

μ—viscosity of fluid, Pa·s,

ρ—density of fluid, kg/m^3,

ρ_0—reference state fluid density, kg/m^3;

ϕ—porosity, %;

ϕ_0—reference state porosity, %.

Subscripts:

i, j, k—grid number;

m—matrix.

References

[1] KLIMKOWSKI L, NAGY S. Key factors in shale gas modeling and simulation. Archives of Mining Sciences, 2014, 59(4): 987–1004.

[2] RUBIN B. Accurate simulation of non-Darcy flow in stimulated fractured shale reservoirs. SPE 132093, 2010.

[3] SAPUTELLI L, LOPEZ C, CHACON A, et al. Design optimization of horizontal wells with multiple hydraulic fractures in the Bakken Shale. SPE 167770, 2014.

[4] MIRZAEI M, CIPOLLA C L. A workflow for modeling and simulation of hydraulic fractures in unconventional gas reservoirs. SPE 153022, 2012.

[5] YAO Jun, WANG Zisheng, ZHANG Yun, et al. Numerical simulation method of discrete fracture network for naturally fractured reservoirs. Acta Petrolei Sinica, 2010, 31(2): 284–288.

[6] HOTEIT H, FIROOZABADI A. Compositional modeling of discrete-fractured media without transfer functions by the discontinuous Galerkin and mixed methods. SPE Journal, 2006, 11(3): 341–352.

[7] MOINFAR A, NARR W, HUI M H, et al. Comparison of discrete-fracture and dual-permeability models for multiphase flow in naturally fractured reservoirs. SPE 142295, 2011.

[8] WEI Yi, RAN Qiquan, LI Ran, et al. Determination of dynamic reserves of fractured horizontal wells in tight oil reservoirs by multi-region material balance method. Petroleum Exploration and Development, 2016, 43(3): 448–455.

[9] KARIMI-FARD M, DURLOFSKY L J, AZIZ K. An efficient discrete-fracture model applicable for general-purpose reservoir simulators. SPE Journal, 2004, 9(2): 227–236.

[10] SANDVE T H, BERRE I, NORDBOTTEN J M. An efficient multi-point flux approximation method for discrete fracture-matrix simulations. Journal of Computational Physics, 2012, 231(9): 3784–3800.

[11] LI Xinning, MA Qiang, LIANG Hui, et al. Geological characteristics and exploration potential of diamictite tight oil in the second Member of the Permian Lucaogou Formation, Santanghu Basin, NW China. Petroleum Exploration and Development, 2015, 42(6): 763–771, 793.

[12] KANG Yili, LI Qiangui, ZHANG Jian, et al. Multi-scale science and the application in oil and gas field development. Journal of Southwest Petroleum University (Science & Technology Edition), 2007, 29(5): 177–180.

[13] ZENG B, CHENG L, LI C. Low velocity non-linear flow in ultra-low permeability reservoir. Journal of Petroleum Science and Engineering, 2011, 80(1): 1–6.

[14] WANG Fei, YUE Xiang'an, WANG Wenliang, et al. Influence of wettability on micro-scale flow and seepage characteristics of simulated crude oil. Acta Petrolei Sinica, 2010, 31(2): 302–305.

[15] YANG Renfeng, JIANG Ruizhong, LIU Shihua, et al. Numerical simulation of nonlinear seepage in ultra-low permeability reservoirs. Acta Petrolei Sinica, 2011, 32(2): 299–306.

[16] PEACEMAN D W. Interpretation of well-block pressures in numerical reservoir simulation with nonsquare grid blocks and anisotropic permeability. SPE Journal, 1983, 23(3): 531–543.

[17] CAUMON G, COLLON-DROUAILLET P, VESLUD C L C D, et al. Surface-based 3D modeling of geological structures. Mathematical Geosciences, 2009, 41(8): 927–945.

[18] MUSTAPHA H. A Gabriel-Delaunay triangulation of 2D complex fractured media for multiphase flow simulations. Computational Geosciences, 2014, 18(6): 989–1008.

[19] JUANES R, SAMPER J, MOLINERO J. A general and efficient formulation of fractures and boundary conditions in the finite element method. International Journal for Numerical Methods in Engineering, 2002, 54(12): 1751–1774.

[20] SANDVE T H. Multiscale simulation of flow and heat transport in fractured geothermal reservoirs. Bergen: University of Bergen, 2012.

[21] LAMPE V. Modelling fluid flow and heat transport in fractured porous media. Bergen: University of Bergen, 2013.

[22] MARGOLIN L G, SHASHKOV M, SMOLARKIEWICZ P K. A discrete operator calculus for finite difference approximations. Computer Methods in Applied Mechanics and Engineering, 2000, 187(3): 365–383.

[23] BONELLE J, ERN A. Analysis of compatible discrete operator schemes for elliptic problems on polyhedral meshes. ESAIM: Mathematical Modelling and Numerical Analysis, 2014, 48(2): 553–581.

[24] LI Xiang, ZHONG Weitao, QIAN Jixin. Automatic differentiation in chemical engineering process optimization. Acta Petrolei Sinica (Petroleum Processing Section), 2001, 17(6): 79–83.

[25] NEIDINGER R D. Introduction to automatic differentiation and MATLAB object-oriented programming. Siam Review, 2010, 52(3): 545–563.